Hybrid Advances 4 (2023) 100088

Contents lists available at ScienceDirect

Hybrid Advances

journal homepage: www.journals.elsevier.com/hybrid-advances

Spray deposited carbon nanotube embedded ZnO as an electrons transport layer in inverted organic solar cells

Anuj Kumar [a], Amanpal Singh [b], Dinesh Kumar [a,c], Ashish Garg [d], Viresh Dutta [e], Sanjay Kumar Swami [f,**], Neha Chaturvedi [g,***], Manoj Kumar [h,*]

[a] Department of Physics, J.C. Bose University of Science and Technology, YMCA, Faridabad, Haryana, 121006, India
[b] Department of Physics, University of Rajasthan, Jaipur, 302004, India
[c] Gurugram University, Gurugram, Haryana, 122003, India
[d] Department of Sustainable Energy Engineering, Indian Institute of Technology Kanpur, Kanpur, 208016, India
[e] Photovoltaic Lab, Department of Energy Science and Engineering, Indian Institute of Technology Delhi, Hauz Khas, New Delhi, 110016, India
[f] CSIR-National Physical Laboratory, Dr. K.S. Krishan Marg, New Delhi, 110016, India
[g] Department of Material Science and Engineering, North Carolina State University, Raleigh, NC, 27695, USA
[h] Department of Physics, School of Physical Sciences, Starex University, Gurugram, Haryana, India

ARTICLE INFO

Keywords:
ZnO
Carbon nanotubes
Spray technique
Inverted organic solar cells

ABSTRACT

In this report, the synthesis and characterization of ZnO and carbon nanotube (CNT) embedded ZnO composite thin films are presented. The obtained ZnO and CNT composite ZnO thin films are used as an electron transport layer (ETL) for bulk heterojunction (BHJ) inverted organic solar cell (IOSC) with the architecture of ITO/ZnO: CNT/PTB7:PC71BM/MoO_3/Ag. Both ZnO and CNT composite ZnO thin films exhibited a highly preferred c-axis oriented (002) diffraction peak and the peak position is shifted toward a lower angle after embedding CNT into the ZnO matrix. The transmittance slightly decreases after CNT is embedded into the ZnO matrix. Completely wrapped CNT with the ZnO was confirmed by Scanning electron microscope (SEM) measurement. The resistivity of ZnO decreased from 2.02×10^{-2} to 5.61×10^{-3} Ω-cm and mobility increased from 4.30 to 15.24 cm^2/V-s after adding CNT into the ZnO matrix. CNT composite ZnO thin film surface is found to be hydrophobic, providing good interfacial contact with the BHJ layer resulting to improve fill factor (FF) of IOSC. The performance of IOSC with CNT composite ZnO ETL layer was significantly improved with a power conversion efficiency of 6.76%, open circuit voltage (V_{OC}) of 700 mV, short circuit current density (J_{SC}) of 20.05 mA/cm^2 and *FF* of 48.17%, respectively.

1. Introduction

Solution-processed organic photovoltaic (OPV) devices based on donor-acceptor (D-A) blended BHJ photoactive layers possess very attractive features such as light weight, flexibility, stretchability, low-cost, and compatibility with large-area and high throughput coating technologies, making it a leading emerging photovoltaic material [1–6]. The power conversion efficiency (PCE) of single junction OPVs has been enhanced by the spin coating process showing a bright future for the application of OPVs to portable and/or wearable consumer goods and building or automotive integration [7]. The current research and fundamental knowledge forged in recent years in the synthesis of efficient donor and acceptor materials for organic solar cells (OSCs) is casting new perspectives in the field. Among a variety of donor polymers, wide band gap region regular polythiophene derivatives and narrow band gap polymers based benzodithiophene (BDI) and thieno thiophene (TT) quinoidal structure have important significance in the course of the development of OSCs [8–11]. Two of the most representative donor polymers are poly (3-hexyl thiophene) (P3HT) and poly [4, 8-bis(5-(2-ethylhexyl) thiophene-2-yl)benzo [1,2-b:4,5-b']dithiophene-co-3-fluorothieno [3,4-b]thiophene-2-carboxylate] (PTB7-Th, also called PCE10, PBDTTT-EF-T, PBDTT-FTTE, etc.) [9].

The current trend of research in solar cells is encouraging and provides the impetus for further focused work not only limited to the

* Corresponding author.
** Corresponding author.
*** Corresponding author.
E-mail addresses: swami.phy@gmail.com (S.K. Swami), nchatur2@ncsu.edu (N. Chaturvedi), panwarm72@gmail.com (M. Kumar).

https://doi.org/10.1016/j.hybadv.2023.100088
Received 31 July 2023; Received in revised form 4 September 2023; Accepted 8 September 2023
Available online 9 September 2023

Table 1
Device performance for solar cells based on ZnO:CNT as an ETL.

Material	J_{SC} (mA/cm^2)	V_{OC} (mV)	*FF* (%)	*PCE* (%)	*Ref.*
ZnO:CNT	9.62	0.56	45.00	2.5	[26]
	14.40	0.75	43.00	4.6	[27]
	14.40	0.53	55.00	4.1	[28]
	16.81	0.72	64.70	7.9	[29]
	18.37	0.79	71.50	10.49	[30]
	17.72	0.80	66.19	9.45	[31]
	21.8	1.03	69.00	15.19	[32]

photoactive layer but also on other key device components where additional losses can occur affecting the performance [12]. The charge transport interlayer(s) is one of such components used to improve the extraction of photo-generated carriers from the BHJ [13]. An ideal interlayer (n-type or p-type) should reduce the recombination losses and also provide considerable processing versatility to ensure layer uniformity while avoiding pinhole formation.

Polymer solar cells with an inverted structure have been proposed to match the vertical component gradient in the active layer and improve its stability compared to conventional device structures based on PEDOT:PSS [11]. It is highly desirable to develop more efficient ETL materials which is one of the most important topics for high-performance devices. To date, there are numerous ETL such as TiO_2, ZnO, SnO_2, etc. are explored that have shown good performance in OSCs due to their excellent processability and semiconductor properties [12–15]. Xiao et al. have studied single-junction solar cells by using a combination of ITO/ZnO and MoO_3/Ag [16]. However, the obstacles have remained to realize scalability and reproducibility based on the solution procession method. Numerous structural defects are generated, and they create a charge recombination path. The ZnO films deposited using a low-temperature solution process formed many intragap states which can trap electrons, resulting the charge transport and interfacial recombination losses [17–19].

By considering this fact, the CNT could be a good choice to solve the problem in order to enhance charge carrier transport and collection phenomena [20–22]. One-dimensional CNTs provide an ideal path for electron transport and guide the charge carriers to be collected by the respected electrodes [23,24]. The interaction between CNTs and ZnO which stuffed the grain boundaries has been utilized to inhibit carrier recombination and improve the device performance [25]. Some of the previous studies using CNT and ZnO in solar cells are listed in Table I.

In the present study, the synthesis and characterization of ZnO and CNT composite ZnO thin films are demonstrated. Inverted organic solar cell using CNT composite ZnO ETL is also presented which exhibited enhanced performance in comparison to ZnO ETL.

2. Experimental details

ZnO and CNT composite ZnO thin films were deposited by using the solution process method on a patterned ITO-coated glass substrate. The patterned ITO substrates were first cleaned in soap solution and then rinsed with de-ionized (DI) water and ultra-sonicated for 15 min in acetone and propanol, respectively. Before deposition, the patterned ITO substrates were put under an ozone lamp to clean the organic and other impurities. The ZnO and CNT incorporated ZnO thin films were deposited on cleaned patterned ITO-coated glass substrates by using the spray pyrolysis method. A precursor solution of 0.3 M zinc acetate with fix amount of CNT 0.05 wt% in methanol was sprayed onto an ITO-coated glass substrate. A Schematic diagram of spray setup is shown in Fig. 1 (a) and also described in detail elsewhere [33]. The ITO-coated glass substrate temperature was maintained at 500 °C during spray deposition and nitrogen gas was used as the carrier gas at a pressure of 1.8 kg/cm^2 and the spray rate was maintained at 1 mL/min.

ZnO and CNT composite ZnO thin films deposited on patterned ITO glass substrate were transferred into nitrogen-filled glove box where the active layer of PTB7:$PC_{71}BM$ was spin-coated at 1000 rpm for 20 s from a solution of concentration 25 mg/mL (1:1.5 wt ratio) prepared in a mixture of a solvent of Di-chlorobenzene and 1, 8 di-iodo-octane (DIO), mixed in a ratio of 97:3 [13]. The active layer coated substrates were left in the glove box environment for the next 1 h to get self-dried. After the drying process, the coated substrates were moved to a thermal evaporator chamber attached to the glove box. Subsequently, MoO_3 and Ag electrodes of 2 and 100 nm thickness were deposited through a shadow mask, respectively. The inverted organic solar cell devices of pixel area 0.09 cm^2 were taken out atan ambient temperature and encapsulated by epoxy under an ozone lamp. The schematic diagram of IOSC is depicted in Fig. 1 (b).

The obtained films were investigated by studying their composition, structural, optical, and electrical properties. X-ray diffraction (Phillips X'PERT PRO) with Cu-Kα radiation was employed to study the crystallographic orientation of the films. Spectral transmittance was recorded in the wavelength range of 300–800 nm by using PerkinElmer Lambda 1050 UV-VIS-NIR spectrophotometer. The surface morphology was observed using a Zeiss EVO-50 SEM. The electrical resistivity of the films was determined by the Van der Pauw Hall effect measurement.

The IOSCs with a pixel area of 0.09 cm^2 were tested under AM 1.5G by Newport solar simulator to measure current density and voltage (*J-V*) characteristics.

3. Results and discussions

The electrical properties of ZnO and CNT composite ZnO thin films were measured by using the Hall Effect measurement. The electrical resistivity of ZnO and CNT composite ZnO thin films was obtained at

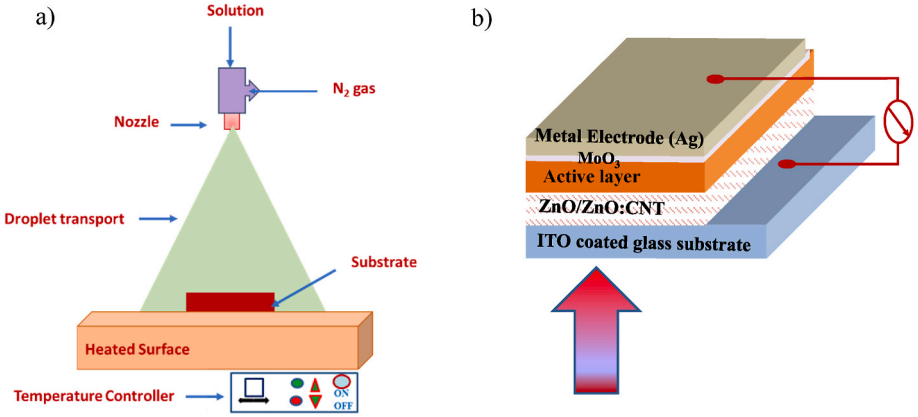

Fig. 1. Schematic diagram of a) Spray setup, b) Inverted organic BHJ solar cell.

Table 2
Electrical properties of ZnO and CNT composite ZnO thin films.

ETL	Resistivity (Ω-cm)	Carrier concentration (cm^{-3})	Mobility (cm^2/V-s)
ZnO	2.02×10^{-2}	7.2×10^{19}	4.30
ZnO: CNT	5.61×10^{-3}	7.31×10^{19}	15.24

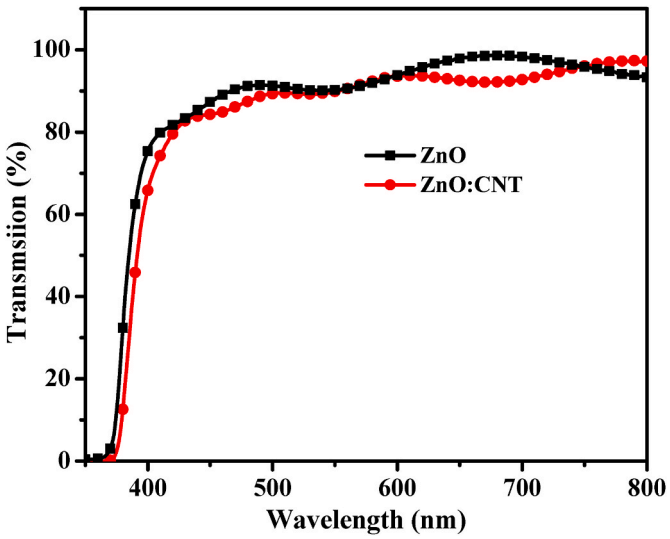

Fig. 2. Transmission spectra of ZnO and CNT composite ZnO thin films.

2.02×10^{-2} and 5.61×10^{-3} Ω-cm, respectively and mobility was observed to be 4.30–15.24 cm^2/V-s, respectively as is listed in Table II. It is found that resistivity decreases and mobility increases drastically after embedding CNT into the ZnO matrix. The cause behind the changed electrical properties of CNT composite ZnO may be due to the grain boundaries stuffed by the CNT, resulting in the boundary potential decreasing and the electron can move easily through the material matrix. Ji Sun Park et al. [34] have suggested that the content of the CNT increases in the composite film and the conductivity is increased due to the CNT providing the proper path to the electrons in the structure. The migration of the electrons from the conduction band of ZnO to the ITO through CNT plays a bridge role. Moreover, CNT is the perfect conductorat room temperature and hence the conductivity of the ZnO matrix increased.

Fig. 2 shows the transmission spectra of ZnO and CNT composite ZnO thin films. It is revealed from the figure that the transmission of the film slightly decreased in the range of 750–600 nm and <500 nm after embedding CNT content into the ZnO matrix. The decrease in the optical transmittance of the film might bedue to the change in absorbance of the CNT composite ZnO thin film which is resulting a change in internal reflectance, absorbance, or surface morphology.

The surface morphology of ZnO and CNT composite ZnO thin films is shown in Fig. 3.

As deposited ZnO film exhibited a smooth and compact structure (Fig. 3a). It is evident from the figure that CNT mixing into the ZnO matrix is observed and is uniformly dispersed in the ZnO matrix (Fig. 3 b). The obtained image revealed that CNTs are completely wrapped with ZnO. It is suggested that CNT enters the matrix of ZnO and affects the optoelectronics properties of ZnO films which further helps in efficient charge transfer while using ZnO as an ETL in IOSC.

An XRD analysis is carried out to study the crystal structure of the fabricated ZnO and CNT-embedded ZnO thin films. The XRD spectrum in Fig. 4 shows only (002) and (004) diffraction peaks at corresponding 2θ angles of 34.99° and 73.29°, respectively (Inset shows XRD pattern of

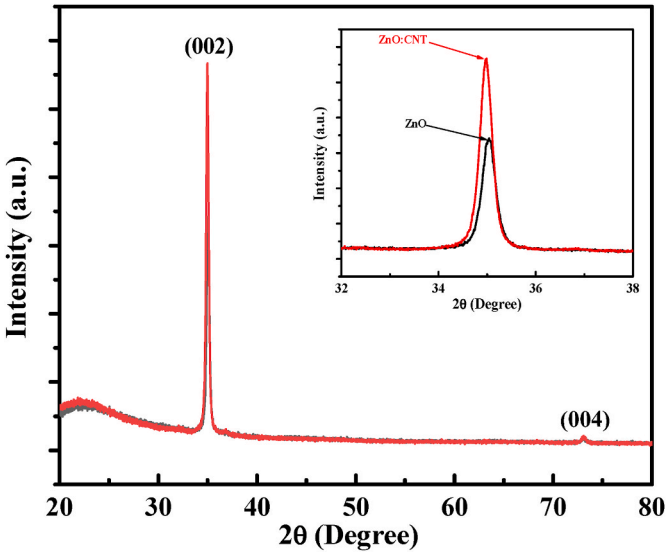

Fig. 4. XRD pattern of ZnO, and CNT composite ZnO thin films.

Table 3
Calculated XRD parameters of spray-deposited ZnO and CNT-embedded ZnO thin films.

Films	(002) peak 2θ (°)	Intensity (CPS)	FWHM (°)	d-spacing (Å)	Crystal size (nm)
ZnO	34.99	44,877	0.31	2.56	28.3
CNT composite ZnO	34.95	76,085	0.28	2.56	30.6

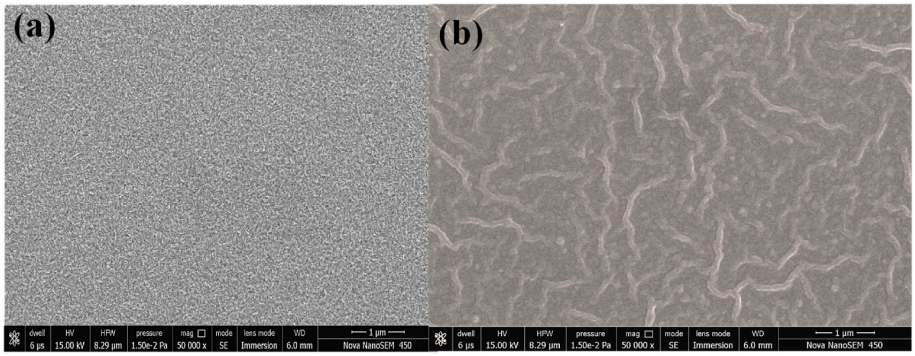

Fig. 3. SEM micrograph for (a) ZnO and (b) CNT composite ZnO thin films.

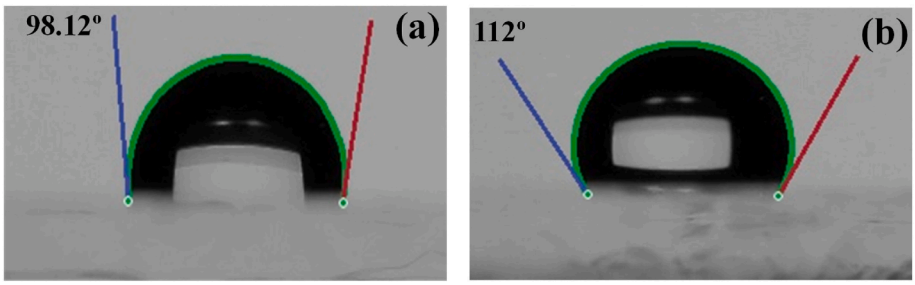

Fig. 5. Contact angle measurement for spray deposited (a) ZnO thin film (b) CNT composite ZnO thin film.

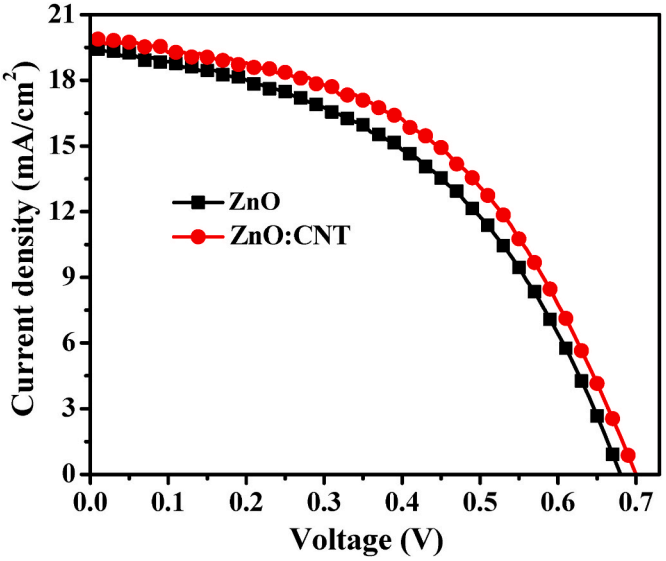

Fig. 6. J-V graph of inverted organic solar cells using ZnO and CNT composite ZnO thin films as ETLs.

CNT embedded ZnO thin film). The obtained pattern is classified wuritze phase of the ZnO and CNT composite ZnO thin films, which is in good agreement with the standard JCPD card. Thus, the resultant planes demonstrated that the hexagonal wuritze ZnO structure was fabricated along with a highly preferred c-axis orientation. The observed crystal structural parameters calculated from the (002) peakare given in Table III.

It is found that the (002) diffraction peak slightly shifts towards a lower angle after adding the CNT in the ZnO matrix indicating that the dopant size is larger than the base material. The grain size was calculated by using Scherr's formula $D = \frac{0.89\,\lambda}{\beta\,cos\,\theta}$. The crystal size of the CNT composite ZnO film increased from 28.3 to 30.6 nm, suggesting the expansion of unit cell volume. As per reported in the literature, CNT enhances the charge transport phenomena in ZnO film in two ways 1) CNT acts as a bridge in the ZnO matrix during the charge transportation and 2) the crystal size increases after adding the CNT into the ZnO matrix as a result a number of grain boundaries suppressed lead to reduce electron scattering during the transportation.

Contact angle measurement was carried out with water to further elucidate the improvement in the performance of CNT-based OSCs. The lower contact angle of 98.12° was observed for ZnO film, indicating its hydrophilic nature, however, the higher contact angle of 112° was detected for CNT composite ZnO thin film shows the hydrophobic nature of the surface (Fig. 5). The hydrophobic surface is beneficial for the intimate contact between ETL and the photoactive layer which leads to enhanced the device performance [35].

Spray-deposited ZnO and CNT-embedded ZnO thin films are used as the electron transport layer in inverted organic solar cells. The *J-V* performance of inverted organic solar cells (ITO/ZnO/PTB7:PC71BM/MoO_3/Ag) fabricated using ZnO and CNT composite ZnO composite thin films as an ETL is shown in Fig. 6.

Table 4
Photovoltaic properties of spray deposited ZnO and CNT composite ZnO ETL-based inverted organic solar cells.

ETL	J_{SC} (mA/cm^2)	V_{OC} (mV)	*FF* (%)	*PCE* (%)
ZnO	19.51	680	45.58	6.05
CNT composite ZnO	20.05	700	48.17	6.76

The IOSC performance in terms of open circuit voltage (V_{OC}), short circuit current density (J_{SC}), fill factor (*FF*), and power conversion efficiency (*PCE*) are presented in Table IV. It is clearly revealed from the obtained results that there is an improvement in the photovoltaic performance after embedding CNT into the ZnO matrix. The observed improvement in the photovoltaic parameters is mainly due to the change in structural morphology, and electrical properties of the ETL after embedding CNT into ZnO thin films.

4. Conclusions

In summary, solution-processed spray deposited bulk heterojunction (BHJ) inverted organic solar cell (IOSC) with the architecture of ITO/ZnO:CNT/PTB7:PC71BM/MoO_3/Ag was successfully developed by utilizing ZnO and CNT composite ZnO thin films as an ETL. Both ETL ZnO and CNT embedded ZnO exhibited highly preferred c-axis orientation (002) diffraction peak. Completely wrapped CNT with the ZnO was confirmed with SEM. The electrical properties were found to be increased after embedding CNT into the ZnO matrix. The hydrophobic nature of CNT composite ZnO ETL improved the interfacial contact for efficient charge transfer. CNT embedded into the ZnO matrix ETL drastically enhanced the device's performance. Such nanocomposite could be useful for the electron transport layer for photovoltaic devices including light emitting devices.

Declaration of competing interest

The authors declare that they have no known competing financial interests or personal relationships that could have appeared to influence the work reported in this paper.

Acknowledgment

Dr. Sanjay Kumar Swami wants to thank the Department of Science and Technology, New Delhi India for INSPIRE Faculty award, and Dr. Anuj Kumar wants to thanks SERB DST Young scientist fellowship and Haryana State Council for Science Innovation and Technology for financial support.

References

[1] P.W.M. Blom, V.D. Mihailetchi, L.J.A. Koster, D.E. Markov, Device physics of polymer:fullerene bulk heterojunction solar cells, Adv. Mater. 19 (2007) 1551–1566, https://doi.org/10.1002/ADMA.200601093.

[2] L.M. Chen, Z. Hong, G. Li, Y. Yang, Recent progress in polymer solar cells: manipulation of polymer:fullerene morphology and the formation of efficient inverted polymer solar cells, Adv. Mater. 21 (2009) 1434–1449, https://doi.org/10.1002/ADMA.200802854.

[3] K. Wei Chou, B. Yan, R. Li, E. Qiang Li, K. Zhao, D.H. Anjum, S. Alvarez, R. Gassaway, A. Biocca, S.T. Thoroddsen, A. Hexemer, A. Amassian, K.W. Chou, B. Yan, R. Li, E.Q. Li, K. Zhao, D.H. Anjum, S.T. Thoroddsen, A. Amassian, S. Alvarez, R. Gassaway, A. Biocca, A. Hexemer, Spin-cast bulk heterojunction solar cells: a dynamical investigation, Adv. Mater. 25 (2013) 1923–1929, https://doi.org/10.1002/ADMA.201203440.

[4] J. Clark, G. Lanzani, Organic photonics for communications, 2010, Nat. Photonics 4 (2010) 438–446, https://doi.org/10.1038/nphoton.2010.160, 7. 4.

[5] S.H. Park, A. Roy, S. Beaupré, S. Cho, N. Coates, J.S. Moon, D. Moses, M. Leclerc, K. Lee, A.J. Heeger, Bulk heterojunction solar cells with internal quantum efficiency approaching 100%, 2009, Nat. Photonics 3 (2009) 297–302, https://doi.org/10.1038/nphoton.2009.69, 5. 3.

[6] K. Vandewal, S. Albrecht, E.T. Hoke, K.R. Graham, J. Widmer, J.D. Douglas, M. Schubert, W.R. Mateker, J.T. Bloking, G.F. Burkhard, A. Sellinger, J.M. J. Fréchet, A. Amassian, M.K. Riede, M.D. McGehee, D. Neher, A. Salleo, Efficient charge generation by relaxed charge-transfer states at organic interfaces, 2013, Nat. Mater. 13 (2013) 63–68, https://doi.org/10.1038/nmat3807, 1. 13.

[7] Y. Cui, Y. Xu, H. Yao, P. Bi, L. Hong, J. Zhang, Y. Zu, T. Zhang, J. Qin, J. Ren, Z. Chen, C. He, X. Hao, Z. Wei, J. Hou, Y. Cui, Y. Xu, H. Yao, P. Bi, L. Hong, Y. Zu, T. Zhang, J. Qin, J. Ren, C. He, J. Hou, Z. Wei, J. Zhang, Z. Chen, X. Hao, Single-junction organic photovoltaic cell with 19% efficiency, Adv. Mater. 33 (2021), 2102420, https://doi.org/10.1002/ADMA.202102420.

[8] T.P. Kaloni, G. Schreckenbach, M.S. Freund, Band gap modulation in polythiophene and polypyrrole-based systems, 2016, Sci. Rep. 6 (2016) 1–18, https://doi.org/10.1038/srep36554, 1. 6.

[9] C. Sih-Hao Liao, H.-J. Jhuo, Y.-S. Cheng, S.-A. Chen, S. Liao, H. Jhuo, Y. Cheng, S. Chen, Fullerene derivative-doped zinc oxide nanofilm as the cathode of inverted polymer solar cells with low-bandgap polymer (PTB7-Th) for high performance, Adv. Mater. 25 (2013) 4766–4771, https://doi.org/10.1002/ADMA.201301476.

[10] Z. He, C. Zhong, S. Su, M. Xu, H. Wu, Y. Cao, Enhanced power-conversion efficiency in polymer solar cells using an inverted device structure, 2012, Nat. Photonics 6 (2012) 591–595, https://doi.org/10.1038/nphoton.2012.190, 9. 6.

[11] N. Chaturvedi, N. Gasparini, D. Corzo, J. Bertrandie, N. Wehbe, J. Troughton, D. Baran, N. Chaturvedi, N. Gasparini, D. Corzo, J. Bertrandie, J.D. Troughton Baran, N. Wehbe, All slot-die coated non-fullerene organic solar cells with PCE 11%, Adv. Funct. Mater. 31 (2021), 2009996 https://doi.org/10.1002/ADFM.202009996.

[12] B. Ecker, H.J. Egelhaaf, R. Steim, J. Parisi, E. von Hauff, Understanding S-shaped current-voltage characteristics in organic solar cells containing a TiO x interlayer with impedance spectroscopy and equivalent circuit analysis, J. Phys. Chem. C 116 (2012) 16333–16337, https://doi.org/10.1021/JP305206D/SUPPL_FILE/JP305206D_SI_001.PDF.

[13] S.K. Swami, N. Chaturvedi, A. Kumar, V. Kumar, A. Garg, V. Dutta, Spray deposited gallium doped zinc oxide (GZO) thin film as the electron transport layer in inverted organic solar cells, Sol. Energy 231 (2022) 458–463, https://doi.org/10.1016/J.SOLENER.2021.12.002.

[14] Z. Liang, Q. Zhang, L. Jiang, G. Cao, ZnO cathode buffer layers for inverted polymer solar cells, Energy Environ. Sci. 8 (2015) 3442–3476, https://doi.org/10.1039/C5EE02510A.

[15] Y. Zhou, J.W. Shim, C. Fuentes-Hernandez, A. Sharma, K.A. Knauer, A.J. Giordano, S.R. Marder, B. Kippelen, Direct correlation between work function of indium-tin-oxide electrodes and solar cell performance influenced by ultraviolet irradiation and air exposure, Phys. Chem. Chem. Phys. 14 (2012) 12014–12021, https://doi.org/10.1039/C2CP42448G.

[16] Z. Xiao, X. Jia, L. Ding, Ternary organic solar cells offer 14% power conversion efficiency, Sci. Bull. 62 (2017) 1562–1564, https://doi.org/10.1016/J.SCIB.2017.11.003.

[17] V. Ischenko, S. Polarz, D. Grote, V. Stavarache, K. Fink, M. Driess, Zinc oxide nanoparticles with defects, Adv. Funct. Mater. 15 (2005) 1945–1954, https://doi.org/10.1002/ADFM.200500087.

[18] L. Nian, W. Zhang, N. Zhu, L. Liu, Z. Xie, H. Wu, F. Würthner, Y. Ma, Photoconductive cathode interlayer for highly efficient inverted polymer solar cells, J. Am. Chem. Soc. 137 (2015) 6995–6998, https://doi.org/10.1021/JACS.5B02168/SUPPL_FILE/JA5B02168_SI_001.PDF.

[19] L. Nian, W. Zhang, S. Wu, L. Qin, L. Liu, Z. Xie, H. Wu, Y. Ma, Perylene bisimide as a promising zinc oxide surface modifier: enhanced interfacial combination for highly efficient inverted polymer solar cells, ACS Appl. Mater. Interfaces 7 (2015) 25821–25827, https://doi.org/10.1021/ACSAMI.5B07759/ASSET/IMAGES/LARGE/AM-2015-07759F_0004.JPEG.

[20] S.N. Habisreutinger, T. Leijtens, G.E. Eperon, S.D. Stranks, R.J. Nicholas, H. J. Snaith, Carbon nanotube/polymer composites as a highly stable hole collection layer in perovskite solar cells, Nano Lett. 14 (2014) 5561–5568, https://doi.org/10.1021/NL501982B/SUPPL_FILE/NL501982B_SI_001.PDF.

[21] L. Communication, W. Yang, W.-F. Leung, L.W.W. Yang, -F. Leung, Electrospun TiO2 nanorods with carbon nanotubes for efficient electron collection in dye-sensitized solar cells, Adv. Mater. 25 (2013) 1792–1795, https://doi.org/10.1002/ADMA.201204256.

[22] W.C. Chang, C.H. Lee, W.C. Yu, C.M. Lin, Optimization of dye adsorption time and film thickness for efficient ZnO dye-sensitized solar cells with high at-rest stability, Nanoscale Res. Lett. 7 (2012) 1–10, https://doi.org/10.1186/1556-276X-7-688/FIGURES/7.

[23] A. du Pasquier, H.E. Unalan, A. Kanwal, S. Miller, M. Chhowalla, Conducting and transparent single-wall carbon nanotube electrodes for polymer-fullerene solar cells, Appl. Phys. Lett. 87 (2005), 203511, https://doi.org/10.1063/1.2132065.

[24] J. Min Lee, J. Sun Park, S. Hwa Lee, H. Kim, S. Yoo, S. Ouk Kim, J.M. Lee, J.S. Park, S.H. Lee, S.O. Kim, H. Kim, S. Yoo, Selective electron- or hole-transport enhancement in bulk-heterojunction organic solar cells with N- or B-doped carbon nanotubes, Adv. Mater. 23 (2011) 629–633, https://doi.org/10.1002/ADMA.201003296.

[25] F. Vietmeyer, B. Seger, P.V. Kamat, Anchoring ZnO particles on functionalized single wall carbon nanotubes. Excited state interactions and charge collection, Adv. Mater. 19 (2007) 2935–2940, https://doi.org/10.1002/ADMA.200602773.

[26] W.H. Shim, S.Y. Park, M.Y. Park, H.O. Seo, K.W. Kim, Y.T. Kim, Y.D. Kim, J. W. Kang, K.H. Lee, Y. Jeong, Y.D. Kim, D.C. Lim, Multifunctional SWCNT-ZnO nanocomposites for enhancing performance and stability of organic solar cells, Adv. Mater. 23 (2011) 519–522, https://doi.org/10.1002/adma.201003083.

[27] S.O. Oseni, K. Kaviyarasu, M. Maaza, G. Sharma, G. Pallicane, G.T. Mola, ZnO:CNT assisted charge transport in PTB7:PCBM blend organic solar cell, J. Alloys Compd. 748 (2018) 216–222, https://doi.org/10.1016/j.jallcom.2018.03.141.

[28] X.G. Mbuyise, E.A.A. Arbab, K. Kaviyarasu, G. Pallicane, M. Maaza, G.T. Mola, Zinc Oxide Doped Single Wall Carbon Nanotubes in Hole Transport Buffer Layer, vol. 706, 2017, pp. 344–350, https://doi.org/10.1016/j.jallcom.2017.02.249.

[29] T. Hu, L. Li, S. Xiao, K. Yuan, H. Yang, L. Chen, Y. Chen, In Situ Implanting Carbon Nanotube-Gold Nanoparticles into ZnO as Efficient Nanohybrid Cathode Buffer Layer for Polymer Solar Cells, vol. 38, 2016, pp. 305–356, https://doi.org/10.1016/j.orgel.2016.09.015.

[30] C. Li, G. Wang, Y. Gao, C. Wang, S. Wen, H. Li, J. Wu, L. Shen, W. Guo, S. Ruan, Highly efficient polymer solar cells based on low-temperature processed ZnO: application of a bifunctional Au@CNTs nanocomposite, J. Mater. Chem. 7 (2019) 2676–2685, https://doi.org/10.1039/C8TC05653F.

[31] S.H. Lee, S.J. Ko, S.H. Eom, H. Kim, D.W. Kim, C. Lee, S.C. Yoon, Composite interlayer consisting of alcohol-soluble polyfluorene and carbon nanotubes for efficient polymer, Sol. Cell. 12 (2020) 14244–14253, https://doi.org/10.1021/acsami.9b22933.

[32] M.K.A. Mohammed, M. Dehghanipour, U. Younis, A.E. Shalan, P. Sakthivel, G. Ravi, P.H. Bhoite, J. Pospisil, Improvement of the Interfacial Contact between Zinc Oxide and a Mixed Cation Perovskite Using Carbon Nanotubes for Ambient-Air-Processed Perovskite Solar Cells, vol. 44, 2020, 19802, https://doi.org/10.1039/D0NJ04656F.

[33] S.K. Swami, N. Chaturvedi, A. Kumar, V. Dutta, Dye sensitized solar cells using the electric field assisted spray deposited kesterite (Cu2ZnSnS4) films as the counter electrodes for improved performance, Electrochim. Acta 263 (2018) 26–33, https://doi.org/10.1016/J.ELECTACTA.2018.01.030.

[34] J.S. Park, J.M. Lee, S.K. Hwang, S.H. Lee, H.J. Lee, B.R. Lee, H. il Park, J.S. Kim, S. Yoo, M.H. Song, S.O. Kim, A ZnO/N-doped carbon nanotube nanocomposite charge transport layer for high performance optoelectronics, J. Mater. Chem. 22 (2012) 12695–12700, https://doi.org/10.1039/C2JM30710C.

[35] S. Fernández, F. Borlaf, F. García-Pérez, M.B. Gómez-Mancebo, C. Munuera, M. García-Hernández, H. Elhouichet, A.F. Braña, F.B. Naranjo, Tailored amorphous ITAZO transparent conductive electrodes, Mater. Sci. Semicond. Process. 90 (2019) 252–258, https://doi.org/10.1016/J.MSSP.2018.10.027.